Published in final edited form as:

Biol Bull. 2016 August ; 231(1): 61–72. doi:10.1086/689591.

Aurora A kinase amplifies a midzone phosphorylation gradient to promote high fidelity cytokinesis

Anna A. Ye[1,2,3], **Julia Torabi**[1,3], and **Thomas J. Maresca**[1,2]

[1]Biology Department, University of Massachusetts, Amherst, Massachusetts, 01003, USA

[2]Molecular and Cellular Biology Graduate Group, University of Massachusetts, Amherst, Massachusetts, 01003, USA

Abstract

Aurora B kinase (ABK) re-localizes from centromeres to the spindle midzone during cytokinesis where it is thought to provide a spatial cue for cytokinesis. While global ABK inhibition in *Drosophila* S2 cells results in macro- and multi-nucleated large cells, mis-localization of midzone ABK (mABK) by depletion of Subito (*Drosophila* MKLP2) does not cause notable cytokinesis defects. Subito depletion was; therefore, used to investigate the contribution of other molecules and redundant pathways to cytokinesis in the absence of mABK. Inhibiting potential polar relaxation pathways via removal of centrosomes (CNN RNAi) or a kinetochore-based phosphatase-gradient (Sds22 RNAi) did not result in cytokinesis defects on their own or in combination with loss of mABK. Disruption of Aurora A kinase (AAK) activity resulted in midzone assembly defects but did not significantly affect contractile ring positioning or cytokinesis. Live-cell imaging of a FRET-based aurora kinase phosphorylation sensor revealed that midzone substrates were less phosphorylated in AAK-inhibited cells, despite the fact that midzone levels of active phosphorylated ABK (pABK) were normal. Interestingly, an increased number of binucleated cells were observed following AAK inhibition in the absence of mABK. The data suggest that equatorial stimulation rather than polar relaxation mechanisms are the major determinants of contractile ring positioning and high-fidelity cytokinesis in *Drosophila* S2 cells. Furthermore, we propose that equatorial stimulation is mediated primarily by the delivery of factors to the cortex by non-centrosomal microtubules (MTs) as well as a midzone-derived phosphorylation gradient that is amplified by the concerted activities of mABK and a soluble pool of AAK.

Introduction

Mitosis is the process in which cells divide their duplicated genetic material into two daughter cells. Equal segregation of the DNA is required for cell viability, thus it is critical that this process is orchestrated flawlessly every time. Cytokinesis is achieved by an actin-myosin contractile ring that physically divides the cell into two daughter cells following separation of the sister chromatids during anaphase. Proper positioning of the contractile

Correspondence to: Thomas J. Maresca, Biology Department, University of Massachusetts, Amherst, Amherst, MA, 01003, Phone: 413-545-0957, Fax: 413-545-3243, tmaresca@bio.umass.edu.

[3]Equal contribution

ring and; hence the cleavage furrow is critically important for cytokinesis but present understanding of the cues that spatially determine where the furrow forms is incomplete.

The Aurora family of proteins is a group of mitotic serine/threonine kinases that regulate many aspects of cell division (Carmena *et al.*, 2009, Hochegger *et al.*, 2013). Aurora A kinase (AAK) and aurora B kinase (ABK), the two members found in *Drosophila melanogaster*, have highly conserved C-terminal kinase domains that phosphorylate many of the same substrates. However, their cellular functions are distinct and dictated by their different cellular localizations, which is determined by the divergent N-terminal regulatory domain (Li *et al.*, 2015). ABK is part of a multi-subunit protein complex called the chromosomal passenger complex (CPC). Prior to anaphase the CPC is highly enriched at the inner centromere and ABK activity contributes to spindle and kinetochore assembly, spindle assembly checkpoint signaling, and error correction (Emanuele *et al.*, 2008, Lampson and Cheeseman, 2011, Moutinho-Pereira *et al.*, 2013, Tanaka *et al.*, 2002). ABK activity is essential for proper cytokinesis (Adams *et al.*, 2001, Echard *et al.*, 2004, Eggert *et al.*, 2004, Smurnyy *et al.*, 2010) and at anaphase onset the CPC complex re-localizes to the spindle midzone (Adams *et al.*, 2000), an area comprised of stable overlapping MTs. The midzone-associated CPC generates an activity gradient (Fuller *et al.*, 2008, Tan and Kapoor, 2011) that helps ensure complete sister chromatid separation (Afonso *et al.*, 2014), and that is proposed to contribute to cleavage furrow positioning (Adams *et al.*, 2000, Tan and Kapoor, 2011, Terada, 2001). Aurora A kinase is required for centrosome maturation, separation and function (Giet *et al.*, 2002, Glover *et al.*, 1995, Hannak *et al.*, 2001), proper kinetochore-MT attachment (Bakhoum *et al.*, 2014, Barisic *et al.*, 2014, Chmatal *et al.*, 2015, Ye *et al.*, 2015), chromosome segregation (Hegarat *et al.*, 2011), MT nucleation (Scrofani *et al.*, 2015) and robust assembly of midzone MTs (Lioutas and Vernos, 2013, Reboutier *et al.*, 2013).

While it is clear that MTs are required for positioning the cleavage furrow (Rappaport, 1971) MT-dependent and MT-independent mechanisms have been proposed to contribute to faithful cytokinesis (Alsop and Zhang, 2003, Canman *et al.*, 2003, Field *et al.*, 2015, Foe and von Dassow, 2008, Murthy and Wadsworth, 2008, Nguyen *et al.*, 2014, Rodrigues *et al.*, 2015). Broadly speaking, two major models are evoked to explain how cells define where the cleavage furrow is positioned during cytokinesis. Equatorial stimulation holds that a positive signal promotes cortical contractility through activation of myosin in between the spindle poles while polar/astral relaxation posits that a signal coming from the vicinity of the spindle poles inhibits contractility causing the polar cortex to relax. While there is evidence that astral MTs in the polar region contribute to polar relaxation (Murthy and Wadsworth, 2008), recent work suggests that the signal does not require astral MTs but rather is mediated by a kinetochore-derived phosphatase gradient (Rodrigues *et al.*, 2015). Equatorial stimulation depends on signals from both the midzone, which is enriched for essential cytokinesis regulators including the CPC (Glotzer, 2005, Nguyen *et al.*, 2014), and an “astral” stimulation signal that requires a sub-population of stable MTs in the vicinity of the furrow site (Canman *et al.*, 2003, Field *et al.*, 2015, Foe and von Dassow, 2008). Thus, three potentially redundant pathways regulate the formation and positioning of the cleavage furrow: (1) polar relaxation, (2) midzone stimulation, and (3) astral stimulation. Here we apply a variety of live-cell imaging techniques in *Drosophila* S2 cells to explore the contribution of each of these pathways to successful cytokinesis.

Materials and Methods

Drosophila S2 cell culture

All cell lines were grown in Schneider's medium (Life Technologies) supplemented with 10% heat inactivated fetal bovine serum (FBS) and 0.5x antibiotic/antimycotic cocktail (Sigma), and maintained in 25°C. All cell lines were generated by transfecting the plasmid with Effectene Transfection Reagent system (Qiagen), following manufacture protocol. Expression of the proteins was checked by fluorescence microscopy. To select the cell expressing the constructs, cells were split in the presence of Blasticidin S HCl (Fisher) and/or Hygromycin (Sigma). Spaghetti Squash (*Dm* MRLC) - GFP, mCherry-α-tubulin cell line was a generous gift from Eric Griffis.

DNA constructs

A soluble FRET based aurora phosphorylation sensor was previously generated (Ye *et al.*, 2015). To target it to MTs, Tau (CG45110) was amplified from cDNA with flanking SpeI sites and inserted into the soluble reporter construct via Gibson assembly (Gibson *et al.*, 2009). The Tau sequence was inserted downstream of the centromere protein C promoter to drive expression of the reporter.

RNAi experiments

DNA templates for subito (CG12298), aurora A kinase (CG3068), Sds22 (CG5851), and CNN (CG4832) were produced to contain ~500 bp of complementary sequence flanked by T7 promoter sequence. dsRNAs were synthesized overnight at 37°C from the DNA templates using the T7 RiboMax Express Large Scale RNA Production System (Promega) following manufacturer protocol. For RNAi experiments, media was aspirated off semi-adhered cell at 25% confluence and replaced with 1ml of serum-free Schneider's medium containing 20μg of dsRNA. After 1h, 1ml of fresh Schneider's plus FBS was added to the wells and incubated for 2 days at 24°C. See Table 1 for primer sequences.

Immunofluorescence

S2 cells were allowed to adhere to acid-washed concanavalin A (Sigma-Aldrich) – coated coverslips, then treated with 5μM MG132 and 125nM MLN8237 (Selleck Chemicals) or DMSO as control for 1 hour before being quickly rinsed with BRB80 and then fixed with 10% paraformaldehyde for 10 minutes. Cells were then permeabilized with PBS containing 1% Triton X-100 for 8 minutes, rinsed three times with PBS plus 0.1% Triton X-100, and blocked with boiled donkey serum for 60 minutes. All primary antibodies were diluted in boiled donkey serum. Anti-Phospho-Aurora A/B/C and Phospho-Aurora A (Cell Signaling Technology) was used at a concentration of 1:1000, DM1α (anti-tubulin antibody; Sigma-Aldrich) at 1:1000. All secondary antibodies (Jackson ImmunoResearch Laboratories, Inc.) were diluted 1:200 in boiled donkey serum. After secondary treatment, coverslips were washed two times with PBS plus 0.1% Triton X-100, followed by incubation with DAPI (1:1000) for 5 minutes, and two additional washes. Cover slips were sealed in mounting media containing 20mM Tris, pH 8.0, 0.5% N-propyl gallate, and 90% glycerol.

Three- or four- color Z series consisting of ~30 planes at 0.2μm intervals were acquired for GFP, Rhodamine, Cy5 (where appropriate), and DAPI channels. Fluorescence intensities were obtained by drawing larger and small regions manually around the maximum intensity projection of the Z-series images. To obtain the ratio intensities, regions were drawn manually on the tubulin channel and transferred to pABK channel. The following equations were used: background signal = (integrated fluorescence intensity of big area – integrated fluorescence intensity of small area)/(big area – small area). Total intensity = integrated fluorescence intensity of small area - (background signal × small area).

FRET

Cells were treated with 125nM MLN8237 or DMSO as control diluted 1:1000, in a tissue culture dish for 1 hour. Cells were allowed to adhere to acid-washed, concanavalin A (Sigma Aldrich) coated coverslip (Corning) for exactly 1 hour, then assembled into a rose chamber containing Schneider's media with 125nM MLN or DMSO, and subjected to imaging at 25°C. Cells were image for a maximum of 1 hour on an eclipse Ti-E inverted microscope (Nikon) equipped with an iXON EMCCD camera (Andor Technology) using a 100x 1.4 NA Plan Apo violet-corrected series differential interference contrast objective (Nikon). Metamorph software (Molecular Devices) was used to control the imaging system.

Mitotic cells were found in the RFP channel, and images of the best focal plane were acquired in RFP, CFP, YFP, and FRET (CFP excitation and YFP emission) channels with equal exposure times. The ratios of the fluorescence intensities of FRET to mTurqoise2 (CFP channel) were obtained by drawing larger and smaller regions in Metamorph (Molecular Devices) around the central spindle in the FRET images and transferred to the CFP image. The following equations were used: background signal = (integrated fluorescence intensity of big area – integrated fluorescence intensity of small area)/(big area – small area). Total intensity = integrated fluorescence intensity of small area - (background signal × small area). The FRET ratio = background corrected total FRET intensity/ background corrected total mTurquoise2 intensity.

Western Blots

A total of 10ug of protein was loaded into a 10% SDS-PAGE gel, run out, and transferred to a nitrocellulose membrane on the Trans-Blot® Turbo™ transfer system (Bio-Rad Laboratories) using the preprogrammed "MIXED MW" 7 minute protocol. All antibodies were diluted in TBS with 0.1% Tween and 5% milk. The membrane was first incubated with anti-Aurora A serum (gift of Marcin Przewloka and David Glover) at 1:5000, followed by DM1α (anti-α-tubulin antibody; Sigma Aldrich) at 1:5000. Rabbit and mouse HRP secondary antibodies (Jackson ImmunoResearch Laboratories, Inc.), diluted at 1:5000, were used in conjunction with their respective primaries and image with a GBox system controlled by GeneSnap software (Syngene).

TIRF and Spinning Disk Confocal Imaging

Cells were allowed to adhere to concanavalin A treated coverslips, and mounted into a rose chamber. Cells were imaged on a TIRF-Spinning Disk system assembled on an Eclipse Ti-E inverted microscope (Nikon) equipped with a Borealis (Andor) retrofitted CSU-10

(Yokogawa) spinning disk head and two ORCA-Flash4.0 LT Digital CMOS camera (Hamamatsu) using a 100x 1.49 NA Apo differential interference contrast objective (Nikon). Metamorph software (Molecular Devices) was used to control the imaging system. Dual TIRF (MRLC-GFP) and widefield (mCherry-α-tubulin) images were acquired at 1 minute intervals. To quantify the myosin dynamic, three 10 pixel^2 boxes were placed in the pole region or the equator, and averaged for each cell. To compare myosin accumulation at the equator and depletion the pole, half maximum change at the equator was normalized to be time 0 for each cell, and 10 before and after time points are reported. For correlative TIRF-spinning disk confocal imaging, cells were followed by time-lapse TIRF imaging and once the cell had assembled a contractile ring (based on MRLC imaging) the system was switched to spinning disk mode and 0.2 μm confocal z-sections were taken. All quantifications and 3D-reconstructions were done using Metamorph (Molecular Devices). Microtubule dynamics in interphase cells were manually tracked using the MTrackJ plug-in (Meijering *et al.*, 2012) in ImageJ (Schneider *et al.*, 2012). The catastrophe and recue frequencies are determined by the number of catastrophe events divided by the total amount of time of time spent polymerizing and the number of rescue events divided by the total amount of time spent depolymerizing, respectively.

Results

To determine if AAK plays a post-metaphase role in *Drosophila* S2 cell division, AAK was knocked down by RNAi, and MT intensity in the spindle midzone during late anaphase was quantified (Fig 1A–C). Consistent with previous reports in other cell types (Lioutas and Vernos, 2013, Reboutier *et al.*, 2013), a 34% decrease in MT midzone population was observed in AAK RNAi depleted cells relative to control cells. Similar to the AAK-depleted conditions, cells treated with a concentration (125 nM) of the inhibitor MLN8237 that specifically inhibits AAK in *Drosophila* S2 cells (Ye *et al.*, 2015), which resulted in loss of pAAK from centrosomes (Fig 1G), exhibited a 40% decrease in midzone MT intensity compared to DMSO-treated cells (Fig 1F–H). The observed decrease in midzone MT density in late anaphase following AAK depletion or chemical inhibition could potentially be a result of inhibiting ABK, as it re-localizes to the overlapping central spindle MTs after anaphase. To examine if the observed results were due to mis-localizing or inhibiting ABK, levels of active phosphorylated ABK (pABK) at midzones were quantified in control and AAK inhibited conditions. When normalized to the control levels, pABK did not exhibit a significant change at the midzone in either AAK knockdown (Fig 1D) or MLN8237-treated cells (Fig 1I) compared to the control conditions. Thus, while the MT intensities were significantly decreased relative to controls in the absence of AAK activity, the total level of midzone pABK was unaffected by either chemical inhibition of AAK or its depletion. It is noteworthy that, while the total amount of pABK did not change, when normalized to the midzone tubulin signal, the amount of midzone pABK per MT increased significantly relative to the controls in both AAK depleted and MLN8237-treated cells (Fig 1E, J).

The midzone aurora kinase activity gradient was next investigated. A FRET based aurora phosphorylation sensor (Fuller *et al.*, 2008, Ye *et al.*, 2015) was generated and targeted to the MTs by fusing it to the MT-associated protein Tau (full length protein). Expression of the Tau-FRET reporter did not obviously bundle MTs nor alter interphase MT dynamics relative

to cells in the same imaging chamber that were not expressing the reporter (Table 2). The sensor is designed such that the FRET ratio decreases when phosphorylated by aurora kinases (Fig 2A). Cells treated with 125nM MLN8237, which specifically inhibits AAK activity and has the same effects as AAK knockdown (Fig 1), exhibited 5% higher FRET emission ratio (Fig 2B, C), indicating that substrates are less phosphorylated by the midzone aurora kinase activity gradient when AAK activity is inhibited in S2 cells despite having normal levels (or even higher levels per MT) of midzone pABK. This finding is consistent with previous work that identified TACC3 and p150Glued as midzone AAK substrates in human cells that were less phosphorylated and mis-localized respectively following AAK inhibition (Lioutas and Vernos, 2013, Reboutier *et al.*, 2013). Importantly, the behavior of a non-phosphorylatable FRET sensor was unaffected by MLN8237 (Fig 2D). We posit that the measured decrease in kinase activity must be due to inhibiting AAK, because pABK levels are actually higher per MT in this condition (Fig 1E, J). Thus we conclude that AAK amplifies a midzone aurora kinase activity gradient.

Where is AAK functionally relevant post-anaphase during midzone assembly and cytokinesis? While we and others have (Berdnik and Knoblich, 2002, Giet *et al.*, 2002, Ye *et al.*, 2015) described the localization pattern of AAK through *Drosophila* cell division, we more closely examined AAK relative to MTs by imaging cells co-expressing mCherry-tagged AAK and GFP-α-tubulin. AAK was highly enriched at centrosomes throughout mitosis and localized to spindle MTs to varying degrees depending on the level of over-expression with a tendency to be enriched near spindle poles in low to moderately expressing cells. In cells with the highest levels of AAK over-expression a slight enrichment of AAK was sometimes observed in the vicinity of kinetochores/centromeres although not to the extent previously seen in mouse oocytes over-expressing AAK (Chmatal *et al.*, 2015). AAK remained enriched at centrosomes throughout anaphase and during cytokinesis although, even in high-expressing cells, AAK only faintly associated with MTs but was not enriched on midzone MTs (Fig. 2E and Supplemental Movie 1). ABK, on the other hand, is highly enriched on midzone MTs and also exhibits MT tip-tracking behavior at anaphase onset when visualized by TIRF microscopy (Vale *et al.*, 2009). We next employed TIRF imaging of cells co-expressing mCherry-tagged AAK and GFP-α-tubulin to determine if AAK exhibited similar behavior as ABK (Fig 2F and Supplemental Movie 2). While AAK was evident at a centrosome that entered the TIRF field during anaphase, it neither tip-tracked nor became enriched on midzone or astral MTs in the cortical region. Thus, we posit that the midzone-derived aurora kinase activity gradient is amplified largely by a soluble rather than MT-associated pool of AAK.

Our data indicate that AAK amplifies a midzone phosphorylation gradient to promote robust midzone assembly in *Drosophila* S2 cells. To examine if the observed defects in midzone assembly impacted furrow formation or assembly of the actin-myosin contractile ring during cytokinesis, myosin dynamics were visualized in living cells expressing GFP-tagged myosin regulatory light chain (MRLC (Spaghetti Squash in *Drosophila))* and mCherry-α-tubulin by TIRF microscopy. In this image-based assay, cells are adhered to Concanavalin A, which prevents successful completion of cytokinesis but allows for impressive visualization of myosin at the cortex after anaphase onset (Vale *et al.*, 2009). In accord with previous TIRF imaging of this cell line (Vale *et al.*, 2009), MRLC was lost from the equator and became

enriched at the site of the cleavage furrow following anaphase onset. There was not a significant difference between DMSO- and MLN8237-treated cells in myosin dynamics at the polar relative to equatorial regions (Fig 2G, H). We next employed correlative TIRF-spinning disk confocal imaging on MLN-treated cells to better observe MRLC organization. A field of cells, which contained a metaphase cell, was imaged by TIRF microscopy for 25 minutes to capture the metaphase cell progress through anaphase, enrich MRLC in the equator and assemble a contractile ring (Supplemental Movie 3). At that point, the field was imaged by confocal spinning disk microscopy (Fig. 2I), 0.2 μm confocal z-sections were acquired (Supplemental Movie 4) and 3D reconstructions were generated for each of the three cells in the field of view (Fig 2 J–L). The cell that progressed from metaphase to anaphase had formed a cleavage furrow and assembled a clear ring of MRLC that deformed the upper part of the midzone (Fig 2J and Supplemental Movie 5). A neighboring cell possessed a midbody and a small ring of MRLC could be seen around the midbody (Fig 2K and Supplemental Movie 6). Since the cells had been treated with MLN for several hours at this point, this cell very likely had progressed through cytokinesis in the absence of AAK activity. An interphase cell with MRLC highly enriched at the cortex contacting the coverslip was also present in the field of view (Fig. 2L and Supplemental Movie 7). Taken together, the data indicate that loss of AAK activity does not dramatically alter MRLC dynamics or organization during cytokinesis.

It is widely accepted that ABK activity is required for cytokinesis and, in support of this, numerous key cytokinesis regulators have been shown to be ABK targets (Adams *et al.*, 2001, Echard *et al.*, 2004, Eggert *et al.*, 2004, Guse *et al.*, 2005, Nunes Bastos *et al.*, 2013, Smurnyy *et al.*, 2010). Similar to the phenotype associated with compromising critical cytokinesis regulators in *Drosophila* such as Pavarotti (*Dm* MKLP1) (Adams *et al.*, 1998), large cells are prevalent following treatment with the *Drosophila* ABK-specific inhibitor Binucleine-2 (Bin2) (Eggert *et al.*, 2004). However, as previously described (Moutinho-Pereira *et al.*, 2013), we have observed that Bin2-treated cells fail to fully condense their chromosomes or assemble bipolar spindles and the spindle assembly checkpoint is severely compromised leading to rapid mitotic exit in the absence of any semblance of normal mitotic timing or organization. Furthermore, while failure in cytokinesis following depletion of bona-fide regulators such as Pavarotti results in cells with two comparably sized nuclei, Bin2-treated cells rarely exhibit the typical binucleate phenotype, but rather have single large nuclei or large nuclei with numerous smaller nuclei. Similar to prior observations (Afonso *et al.*, 2014), Bin2 addition in early anaphase led to rapid mitotic exit and the formation of a single large nucleus (Fig 3A, Supplemental Movies 8, 9). The fact that this Bin2-treated anaphase cell did not complete cytokinesis is likely due to the consequences of rapid mitotic exit as well as the positioning of the nucleus in the midzone position. Thus, the pleiotropic effects of globally inhibiting ABK make cytokinesis defects difficult to interpret. To better isolate the contribution of midzone ABK (mABK), the *Drosophila* MKLP2 homologue Subito, which has been shown to localize CPC to the midzone in numerous model systems including *Drosophila* (Cesario *et al.*, 2006, Gruneberg *et al.*, 2004, Nguyen *et al.*, 2014), was depleted by RNAi. Subito depletion resulted in a substantial reduction in midzone levels of pABK (Fig 3B, C). Mis-localizing mABK by Subito depletion did not result in a significant increase in the number of binucleated cells compared to control

conditions (Fig 3 D). While AAK contributes to the midzone phosphorylation gradient, the frequency of binucleated cells was not increased in MLN-treated cells relative to DMSO controls (Fig 3 D). We reasoned that if AAK amplifies the midzone activity gradient to promote cytokinesis, then inhibition of AAK in the absence of mABK would result in a higher frequency of cytokinesis failure. Indeed, MLN-treated cells depleted of mABK resulted in a ~4 fold increase in binucleate cells compared to controls (Fig 3D). The additive effect of losing both AAK and mABK activities suggests that the two kinases work together to increase the fidelity of cytokinesis. In the double inhibited cells, the midzone aurora kinase activity gradient is compromised and while a 4-fold increase in cytokinesis failure is not desirable, most cells manage to complete cytokinesis. Thus, redundant pathways must compensate for the loss of the midzone aurora phosphorylation gradient.

Previous work has shown that a kinetochore-based PP1-Sds22 phosphatase gradient mediates the polar relaxation signal (Kunda *et al.*, 2012, Rodrigues *et al.*, 2015). To inhibit the relaxation gradient and examine its functional redundancy with the equatorial stimulation signal from aurora kinases, Sds22 was depleted from cells alone and in combination with treatments that disrupt the midzone aurora kinase activity gradient. As previously reported (Rodrigues *et al.*, 2015), depletion of Sds22 did not lead to a measurable increase in cytokinesis failure (Fig 3E). Interestingly, cells lacking Sds22 in which AAK was also inhibited were no more prone to fail cytokinesis than control cells while Sds22 depletion combined with loss of the midzone aurora kinase activity gradient were indistinguishable from Subito-depleted cells treated with 125nM MLN8237 (Fig 3D, E). Thus, Sds22-dependent polar relaxation is dispensable for proper cytokinesis even in the absence of the aurora-mediated equatorial stimulation signal. Astral MTs, presumably derived from centrosomes, have been proposed to contribute to both polar relaxation (Murthy and Wadsworth, 2008) and equatorial stimulation (Rappaport, 1961). Centrosomin (CNN) was depleted to examine the contribution of centrosome-derived astral MTs to cytokinesis and their redundancy with the midzone aurora phosphorylation gradient. In CNN RNAi cells treated with either DMSO or MLN8237, the percentage of binucleated cells was not different from control cells (Fig 3F). As was the case for Sds22 depletion, CNN depletion in combination with Subito RNAi and 125nM MLN8237 exhibited the same phenotype as cells lacking mABK and AAK activity (Fig 3D–F), suggesting that centrosomal MTs do not make a major contribution to cytokinesis in *Drosophila* S2 cells even when the midzone aurora kinase activity gradient is compromised.

Discussion

The aurora family kinases regulate many mitotic pathways and their critical functions in early mitosis make it difficult to study their involvements in late anaphase and cytokinesis. Lioutas et al, and Reboutier et al. have reported the importance of AAK in formation of a central spindle by regulating MT growth through phosphorylation of TACC3 and p150Glued, respectively (Lioutas and Vernos, 2013, Reboutier *et al.*, 2013). Here we report that AAK activity also contributes to robust midzone MT assembly and contributes to phosphorylation of midzone substrates in *Drosophila* S2 cells. Interestingly, total midzone levels of pABK were normal in AAK inhibited cells and actually higher when ratioed to MTs despite having less robust midzones. Thus, there may be a regulatory mechanism that

ensures adequate levels of CPC enrichment at overlapping midzone MTs that buffers against variations in MT density.

The experiments conducted in this study have allowed us to dissect the contributions of equatorial stimulation and polar relaxation pathways (Fig 3G). While depletion of MKLP2 and Subito leads to loss of mABK in both human and *Drosophila* cells respectively, its depletion leads to a significantly higher incidence of cytokinesis failure in human cells (Kitagawa *et al.*, 2014, Kitagawa *et al.*, 2013, Zhu *et al.*, 2005). Since MKLP2-depleted cells fail during the late stages of cytokinesis (Zhu *et al.*, 2005), this discrepancy may be due to differences in abscission mechanisms between human and *Drosophila*. Interestingly, the fact that the cleavage furrow ingresses between segregating chromosomes in MKLP2-depleted human cells suggests that, like in *Drosophila* S2 cells, mABK is likely dispensable for spatially positioning the cleavage furrow in human cells as well. In *Drosophila*, both midzone-derived and astral stimulation signals likely contribute to equatorial stimulation while recent work suggests that polar relaxation is mediated by a phosphatase gradient emanating from kinetochores. We have shown that a midzone-based aurora kinase activity gradient that requires both mABK and a predominantly soluble pool of AAK contributes to the fidelity of cytokinesis. However, redundant and/or dominant pathways must exist since a majority of cells lacking the midzone aurora activity gradient successfully complete cytokinesis. Polar relaxation signals from the phosphatase gradient or by centrosomal MTs are neither dominant since single depletions of Sds22 or CNN do not lead to cytokinesis defects, nor redundant to the midzone aurora kinase activity gradient since the effects of depleting CNN or Sds22 combined with loss of the aurora phosphorylation gradient was identical to removing the aurora activity gradient alone. We infer from these data that the dominant pathway for spatially defining furrow formation in *Drosophila* S2 cells is the astral stimulation pathway.

Interestingly, astral stimulation, in this case, does not require centrosome-derived MTs since CNN depletion has no effect on cytokinesis. We acknowledge that the concept of “astral” MTs without centrosomes seems counter-intuitive; however, we propose that in *Drosophila* S2 cells (what is historically referred to as) the astral stimulation pathway is actually mediated by a population of critically important “furrow MTs” that do not require centrosomes to assemble. Furthermore, since inhibiting Pavarotti (*Dm* MKLP1) in *Drosophila* cells leads to complete failure in cytokinesis (Adams *et al.*, 1998, Echard *et al.*, 2004, Eggert *et al.*, 2004, Goshima and Vale, 2003) it is likely that Pavarotti, as part of the Centralspindlin complex with RacGAP50C (*Dm* MgcRacGAP) (Glotzer, 2005) and other regulatory components, at the ends of furrow MTs are the central determinants of where the cleavage furrow forms. Pavarotti has been observed to tip-track on MTs at anaphase onset and eventually concentrates on the ends of MTs in the vicinity of the furrow where it bundles and stabilizes intersecting MTs in the equatorial region (Vale *et al.*, 2009). Both Pavarotti and ABK have also been shown to accumulate as a band at the equatorial cortex distinct from their localization to cortical MTs (Hu *et al.*, 2008, 2011, Minestrini *et al.*, 2003, Vale *et al.*, 2009). Like Pavarotti, ABK, which has been reported to phosphorylate and regulate MKLP1 (Guse *et al.*, 2005), accumulates on MT plus-ends at anaphase onset and inhibition of ABK blocked the equatorial accumulation but not the tip-localizing behavior of Pavarotti (Vale *et al.*, 2009). We envision that a midzone-derived aurora kinase activity

gradient contributes to cytokinesis via crosstalk with a more dominant astral stimulation/furrow MT pathway through multiple non mutually-exclusive mechanisms: 1) phosphorylating tip-tracking regulatory complexes, 2) rendering cortical components competent for equatorial accumulation of cytokinesis regulators such as RhoA, RhoGEF, ABK, and Pavarotti, and 3) stabilization of furrow MTs, for example, through inhibition of catastrophe factors (Gadea and Ruderman, 2006, Kelly *et al.*, 2007, Sampath *et al.*, 2004). In conclusion, we favor a model in which furrow positioning in *Drosophila* S2 cells is driven largely by equatorial stimulation that is comprised of 1) a midzone-derived stimulation signal to which an aurora kinase activity gradient contributes and 2) what has traditionally been referred to as an "astral" stimulation signal, that is mediated by a non-centrosomal population of stable furrow MTs in the vicinity of the equatorial cortex (Canman *et al.*, 2003, Field *et al.*, 2015, Foe and von Dassow, 2008).

Supplementary Material

Refer to Web version on PubMed Central for supplementary material.

Acknowledgments

We would like to thank Eric Griffis for generously providing *Drosophila* S2 cell lines, and Marcin Przewloka and David Glover for the generous gift of the *Drosophila* anti-Aurora A. We are also grateful to Pat Wadsworth for sharing many insightful discussions on cytokinesis. This work was supported by an NIH grant (5 R01 GM107026) to T.J.M and by Research Grant No. 5-FY13-205 from the March of Dimes Foundation to T.J.M, as well as support from the Charles H. Hood Foundation, Inc., Boston, MA. to T.J.M.

Abbreviations

AAK	Aurora A Kinase
ABK	Aurora B Kinase
CNN	Centrosomin
CPC	Chromosomal Passenger Complex
FRET	Förster (or Fluorescence) Resonance Energy Transfer
GFP	Green Fluorescent Protein
MT	Microtubule
MKLP1	Mitotic Kinesin-Like Protein 1
MKLP2	Mitotic Kinesin-Like Protein 2
MRLC	Myosin Regulatory Light Chain
pAAK	phospho-Aurora A kinase
pABK	phospho-Aurora B kinase
RFP	Red Fluorescent Protein

TACC3 Transforming, Acidic Coiled-Coil Containing Protein 3

References

Adams RR, Maiato H, Earnshaw WC, Carmena M. Essential roles of Drosophila inner centromere protein (INCENP) and aurora B in histone H3 phosphorylation, metaphase chromosome alignment, kinetochore disjunction, and chromosome segregation. J Cell Biol. 2001; 153:865–880. [PubMed: 11352945]

Adams RR, Tavares AA, Salzberg A, Bellen HJ, Glover DM. pavarotti encodes a kinesin-like protein required to organize the central spindle and contractile ring for cytokinesis. Genes Dev. 1998; 12:1483–1494. [PubMed: 9585508]

Adams RR, Wheatley SP, Gouldsworthy AM, Kandels-Lewis SE, Carmena M, Smythe C, Gerloff DL, Earnshaw WC. INCENP binds the Aurora-related kinase AIRK2 and is required to target it to chromosomes, the central spindle and cleavage furrow. Curr Biol. 2000; 10:1075–1078. [PubMed: 10996078]

Afonso O, Matos I, Pereira AJ, Aguiar P, Lampson MA, Maiato H. Feedback control of chromosome separation by a midzone Aurora B gradient. Science. 2014; 345:332–336. [PubMed: 24925910]

Alsop GB, Zhang D. Microtubules are the only structural constituent of the spindle apparatus required for induction of cell cleavage. J Cell Biol. 2003; 162:383–390. [PubMed: 12900392]

Bakhoum SF, Kabeche L, Murnane JP, Zaki BI, Compton DA. DNA-damage response during mitosis induces whole-chromosome missegregation. Cancer Discov. 2014; 4:1281–1289. [PubMed: 25107667]

Barisic M, Aguiar P, Geley S, Maiato H. Kinetochore motors drive congression of peripheral polar chromosomes by overcoming random arm-ejection forces. Nat Cell Biol. 2014; 16:1249–1256. [PubMed: 25383660]

Berdnik D, Knoblich JA. Drosophila Aurora-A is required for centrosome maturation and actin-dependent asymmetric protein localization during mitosis. Curr Biol. 2002; 12:640–647. [PubMed: 11967150]

Canman JC, Cameron LA, Maddox PS, Straight A, Tirnauer JS, Mitchison TJ, Fang G, Kapoor TM, Salmon ED. Determining the position of the cell division plane. Nature. 2003; 424:1074–1078. [PubMed: 12904818]

Carmena M, Ruchaud S, Earnshaw WC. Making the Auroras glow: regulation of Aurora A and B kinase function by interacting proteins. Curr Opin Cell Biol. 2009; 21:796–805. [PubMed: 19836940]

Cesario JM, Jang JK, Redding B, Shah N, Rahman T, McKim KS. Kinesin 6 family member Subito participates in mitotic spindle assembly and interacts with mitotic regulators. J Cell Sci. 2006; 119:4770–4780. [PubMed: 17077127]

Chmatal L, Yang K, Schultz RM, Lampson MA. Spatial Regulation of Kinetochore Microtubule Attachments by Destabilization at Spindle Poles in Meiosis I. Curr Biol. 2015; 25:1835–1841. [PubMed: 26166779]

Echard A, Hickson GR, Foley E, O'Farrell PH. Terminal cytokinesis events uncovered after an RNAi screen. Curr Biol. 2004; 14:1685–1693. [PubMed: 15380073]

Eggert US, Kiger AA, Richter C, Perlman ZE, Perrimon N, Mitchison TJ, Field CM. Parallel chemical genetic and genome-wide RNAi screens identify cytokinesis inhibitors and targets. PLoS Biol. 2004; 2:e379. [PubMed: 15547975]

Emanuele MJ, Lan W, Jwa M, Miller SA, Chan CS, Stukenberg PT. Aurora B kinase and protein phosphatase 1 have opposing roles in modulating kinetochore assembly. J Cell Biol. 2008; 181:241–254. [PubMed: 18426974]

Field CM, Groen AC, Nguyen PA, Mitchison TJ. Spindle-to-cortex communication in cleaving, polyspermic Xenopus eggs. Mol Biol Cell. 2015; 26:3628–3640. [PubMed: 26310438]

Foe VE, von Dassow G. Stable and dynamic microtubules coordinately shape the myosin activation zone during cytokinetic furrow formation. J Cell Biol. 2008; 183:457–470. [PubMed: 18955555]

Fuller BG, Lampson MA, Foley EA, Rosasco-Nitcher S, Le KV, Tobelmann P, Brautigan DL, Stukenberg PT, Kapoor TM. Midzone activation of aurora B in anaphase produces an intracellular phosphorylation gradient. Nature. 2008; 453:1132–1136. [PubMed: 18463638]

Gadea BB, Ruderman JV. Aurora B is required for mitotic chromatin-induced phosphorylation of Op18/Stathmin. Proc Natl Acad Sci U S A. 2006; 103:4493–4498. [PubMed: 16537398]

Gibson DG, Young L, Chuang RY, Venter JC, Hutchison CA 3rd, Smith HO. Enzymatic assembly of DNA molecules up to several hundred kilobases. Nat Methods. 2009; 6:343–345. [PubMed: 19363495]

Giet R, McLean D, Descamps S, Lee MJ, Raff JW, Prigent C, Glover DM. Drosophila Aurora A kinase is required to localize D-TACC to centrosomes and to regulate astral microtubules. J Cell Biol. 2002; 156:437–451. [PubMed: 11827981]

Glotzer M. The molecular requirements for cytokinesis. Science. 2005; 307:1735–1739. [PubMed: 15774750]

Glover DM, Leibowitz MH, McLean DA, Parry H. Mutations in aurora prevent centrosome separation leading to the formation of monopolar spindles. Cell. 1995; 81:95–105. [PubMed: 7720077]

Goshima G, Vale RD. The roles of microtubule-based motor proteins in mitosis: comprehensive RNAi analysis in the Drosophila S2 cell line. J Cell Biol. 2003; 162:1003–1016. [PubMed: 12975346]

Gruneberg U, Neef R, Honda R, Nigg EA, Barr FA. Relocation of Aurora B from centromeres to the central spindle at the metaphase to anaphase transition requires MKlp2. J Cell Biol. 2004; 166:167–172. [PubMed: 15263015]

Guse A, Mishima M, Glotzer M. Phosphorylation of ZEN-4/MKLP1 by aurora B regulates completion of cytokinesis. Curr Biol. 2005; 15:778–786. [PubMed: 15854913]

Hannak E, Kirkham M, Hyman AA, Oegema K. Aurora-A kinase is required for centrosome maturation in Caenorhabditis elegans. J Cell Biol. 2001; 155:1109–1116. [PubMed: 11748251]

Hegarat N, Smith E, Nayak G, Takeda S, Eyers PA, Hochegger H. Aurora A and Aurora B jointly coordinate chromosome segregation and anaphase microtubule dynamics. J Cell Biol. 2011; 195:1103–1113. [PubMed: 22184196]

Hochegger H, Hegarat N, Pereira-Leal JB. Aurora at the pole and equator: overlapping functions of Aurora kinases in the mitotic spindle. Open Biol. 2013; 3:120185. [PubMed: 23516109]

Hu CK, Coughlin M, Field CM, Mitchison TJ. Cell polarization during monopolar cytokinesis. J Cell Biol. 2008; 181:195–202. [PubMed: 18411311]

Hu CK, Coughlin M, Field CM, Mitchison TJ. KIF4 regulates midzone length during cytokinesis. Curr Biol. 2011; 21:815–824. [PubMed: 21565503]

Kelly AE, Sampath SC, Maniar TA, Woo EM, Chait BT, Funabiki H. Chromosomal enrichment and activation of the aurora B pathway are coupled to spatially regulate spindle assembly. Dev Cell. 2007; 12:31–43. [PubMed: 17199039]

Kitagawa M, Fung SY, Hameed UF, Goto H, Inagaki M, Lee SH. Cdk1 coordinates timely activation of MKlp2 kinesin with relocation of the chromosome passenger complex for cytokinesis. Cell Rep. 2014; 7:166–179. [PubMed: 24656812]

Kitagawa M, Fung SY, Onishi N, Saya H, Lee SH. Targeting Aurora B to the equatorial cortex by MKlp2 is required for cytokinesis. PLoS One. 2013; 8:e64826. [PubMed: 23750214]

Kunda P, Rodrigues NT, Moeendarbary E, Liu T, Ivetic A, Charras G, Baum B. PP1-mediated moesin dephosphorylation couples polar relaxation to mitotic exit. Curr Biol. 2012; 22:231–236. [PubMed: 22209527]

Lampson MA, Cheeseman IM. Sensing centromere tension: Aurora B and the regulation of kinetochore function. Trends Cell Biol. 2011; 21:133–140. [PubMed: 21106376]

Li S, Deng Z, Fu J, Xu C, Xin G, Wu Z, Luo J, Wang G, Zhang S, Zhang B, Zou F, Jiang Q, Zhang C. Spatial compartmentalization specializes function of Aurora-A and Aurora-B. J Biol Chem. 2015

Lioutas A, Vernos I. Aurora A kinase and its substrate TACC3 are required for central spindle assembly. EMBO Rep. 2013; 14:829–836. [PubMed: 23887685]

Meijering E, Dzyubachyk O, Smal I. Methods for cell and particle tracking. Methods Enzymol. 2012; 504:183–200. [PubMed: 22264535]

Minestrini G, Harley AS, Glover DM. Localization of Pavarotti-KLP in living Drosophila embryos suggests roles in reorganizing the cortical cytoskeleton during the mitotic cycle. Mol Biol Cell. 2003; 14:4028–4038. [PubMed: 14517316]

Moutinho-Pereira S, Stuurman N, Afonso O, Hornsveld M, Aguiar P, Goshima G, Vale RD, Maiato H. Genes involved in centrosome-independent mitotic spindle assembly in Drosophila S2 cells. Proc Natl Acad Sci U S A. 2013; 110:19808–19813. [PubMed: 24255106]

Murthy K, Wadsworth P. Dual role for microtubules in regulating cortical contractility during cytokinesis. J Cell Sci. 2008; 121:2350–2359. [PubMed: 18559890]

Nguyen PA, Groen AC, Loose M, Ishihara K, Wuhr M, Field CM, Mitchison TJ. Spatial organization of cytokinesis signaling reconstituted in a cell-free system. Science. 2014; 346:244–247. [PubMed: 25301629]

Nunes Bastos R, Gandhi SR, Baron RD, Gruneberg U, Nigg EA, Barr FA. Aurora B suppresses microtubule dynamics and limits central spindle size by locally activating KIF4A. J Cell Biol. 2013; 202:605–621. [PubMed: 23940115]

Rappaport R. Experiments concerning the cleavage stimulus in sand dollar eggs. J Exp Zool. 1961; 148:81–89. [PubMed: 14490383]

Rappaport R. Cytokinesis in animal cells. Int Rev Cytol. 1971; 31:169–213. [PubMed: 4400359]

Reboutier D, Troadec MB, Cremet JY, Chauvin L, Guen V, Salaun P, Prigent C. Aurora A is involved in central spindle assembly through phosphorylation of Ser 19 in P150Glued. J Cell Biol. 2013; 201:65–79. [PubMed: 23547029]

Rodrigues NT, Lekomtsev S, Jananji S, Kriston-Vizi J, Hickson GR, Baum B. Kinetochore-localized PP1-Sds22 couples chromosome segregation to polar relaxation. Nature. 2015; 524:489–492. [PubMed: 26168397]

Sampath SC, Ohi R, Leismann O, Salic A, Pozniakovski A, Funabiki H. The chromosomal passenger complex is required for chromatin-induced microtubule stabilization and spindle assembly. Cell. 2004; 118:187–202. [PubMed: 15260989]

Schneider CA, Rasband WS, Eliceiri KW. NIH Image to ImageJ: 25 years of image analysis. Nat Methods. 2012; 9:671–675. [PubMed: 22930834]

Scrofani J, Sardon T, Meunier S, Vernos I. Microtubule nucleation in mitosis by a RanGTP-dependent protein complex. Curr Biol. 2015; 25:131–140. [PubMed: 25532896]

Smurnyy Y, Toms AV, Hickson GR, Eck MJ, Eggert US. Binucleine 2, an isoform-specific inhibitor of Drosophila Aurora B kinase, provides insights into the mechanism of cytokinesis. ACS Chem Biol. 2010; 5:1015–1020. [PubMed: 20804174]

Tan L, Kapoor TM. Examining the dynamics of chromosomal passenger complex (CPC)-dependent phosphorylation during cell division. Proc Natl Acad Sci U S A. 2011; 108:16675–16680. [PubMed: 21949386]

Tanaka TU, Rachidi N, Janke C, Pereira G, Galova M, Schiebel E, Stark MJ, Nasmyth K. Evidence that the Ipl1-Sli15 (Aurora kinase-INCENP) complex promotes chromosome bi-orientation by altering kinetochore-spindle pole connections. Cell. 2002; 108:317–329. [PubMed: 11853667]

Terada Y. Role of chromosomal passenger complex in chromosome segregation and cytokinesis. Cell Struct Funct. 2001; 26:653–657. [PubMed: 11942622]

Vale RD, Spudich JA, Griffis ER. Dynamics of myosin, microtubules, and Kinesin-6 at the cortex during cytokinesis in Drosophila S2 cells. J Cell Biol. 2009; 186:727–738. [PubMed: 19720876]

Ye AA, Deretic J, Hoel CM, Hinman AW, Cimini D, Welburn JP, Maresca TJ. Aurora A Kinase Contributes to a Pole-Based Error Correction Pathway. Curr Biol. 2015; 25:1842–1851. [PubMed: 26166783]

Zhu C, Zhao J, Bibikova M, Leverson JD, Bossy-Wetzel E, Fan JB, Abraham RT, Jiang W. Functional analysis of human microtubule-based motor proteins, the kinesins and dyneins, in mitosis/cytokinesis using RNA interference. Mol Biol Cell. 2005; 16:3187–3199. [PubMed: 15843429]

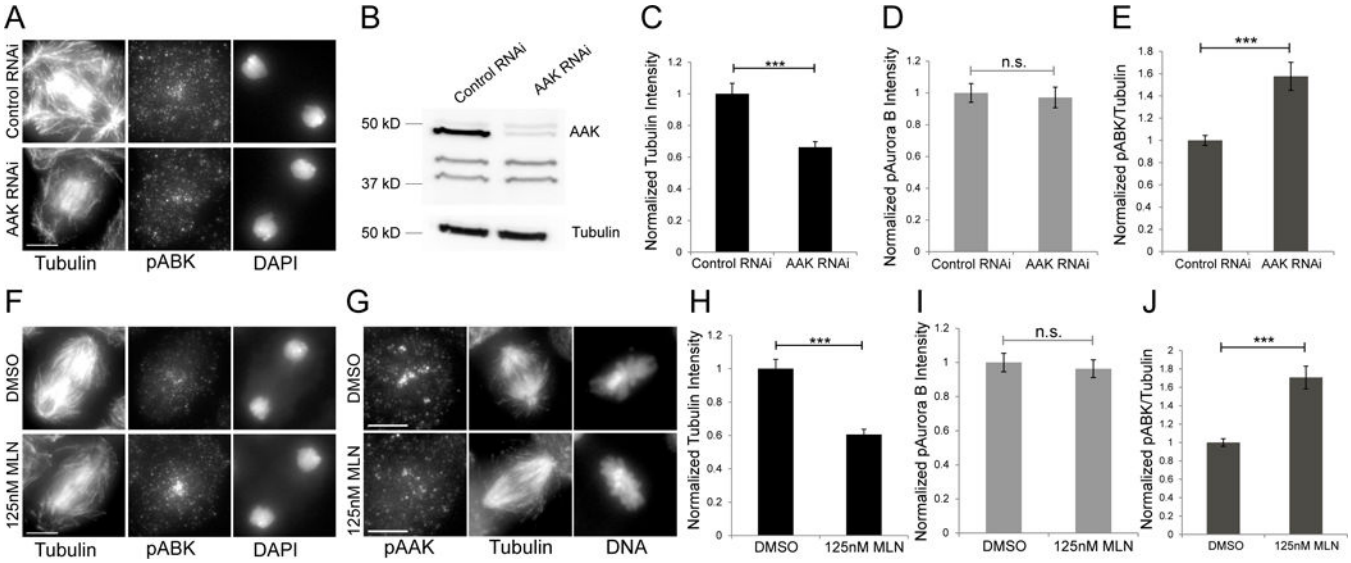

Figure 1. Aurora A is required for robust midzone assembly but its inhibition does not mis-localize phospho-ABK

(A) Representative images of control- and AAK RNAi cells showing a decrease in MT intensity in AAK depleted cells. **(B)** AAK can be efficiently depleted from S2 cells as assayed by western blot analysis of control and AAK RNAi cells. Tubulin was used as the loading control. **(C)** Quantification of midzone MT intensity normalized to control RNAi. Midzone MT density is significantly decreased in late anaphase/telophase cells lacking AAK activity. Quantifications are from 2 independent experiments. Control RNAi; n = 62 cells, AAK RNAi; n = 70 cells. **(D)** AAK depletion does not change the total amount of midzone-associated phosphorylated ABK (pABK). Quantifications are from 2 independent experiments. Control RNAi; n = 62 cells, AAK RNAi; n = 70 cells. **(E)** AAK depletion leads to more pABK per MT in the central spindle. Quantifications are from 2 independent experiments. Control RNAi; n = 62 cells, AAK RNAi; n = 70 cells. **(F)** Representative images of DMSO- and 125nM MLN8237 treated cells showing a decrease in midzone MT intensity in the AAK inhibited cell relative to the control cell. **(G)** Representative images of cells treated with DMSO (top) or 125nM MLN8237 (bottom), stained with anti-phospho-AAK (pAAK). Cells treated with MLN8237 do not have pAAK staining at centrosomes. We previously demonstrated (Ye *et al.*, 2015) that the apparent centromere staining with the anti-pAAK antibody is due to cross-reactivity with pABK. **(H)** Cells treated with 125nM MLN8237 phenocopy AAK depleted cells, exhibiting decreased MT density in the spindle midzone. Quantifications are from 2 independent experiments. DMSO; n = 77 cells. 125nM MLN8237; n = 77 cells. **(I)** 125nM MLN8237 does not decrease total pABK localization to the midzone. Quantifications are from 2 independent experiments. DMSO; n = 77 cells. 125nM MLN8237; n = 77 cells. **(J)** Cells treated with 125nM MLN phenocopies cells depleted of AAK, having more pABK per MT. Quantifications are from 2 independent experiments. DMSO; n = 77 cells. 125nM MLN8237; n = 77 cells. Error bars are SEM. Scale bars are 5μm. Two-tailed Student's t-tests are reported: not significant (n.s.) = p-value > 0.05, *** = p-value < 0.0005.

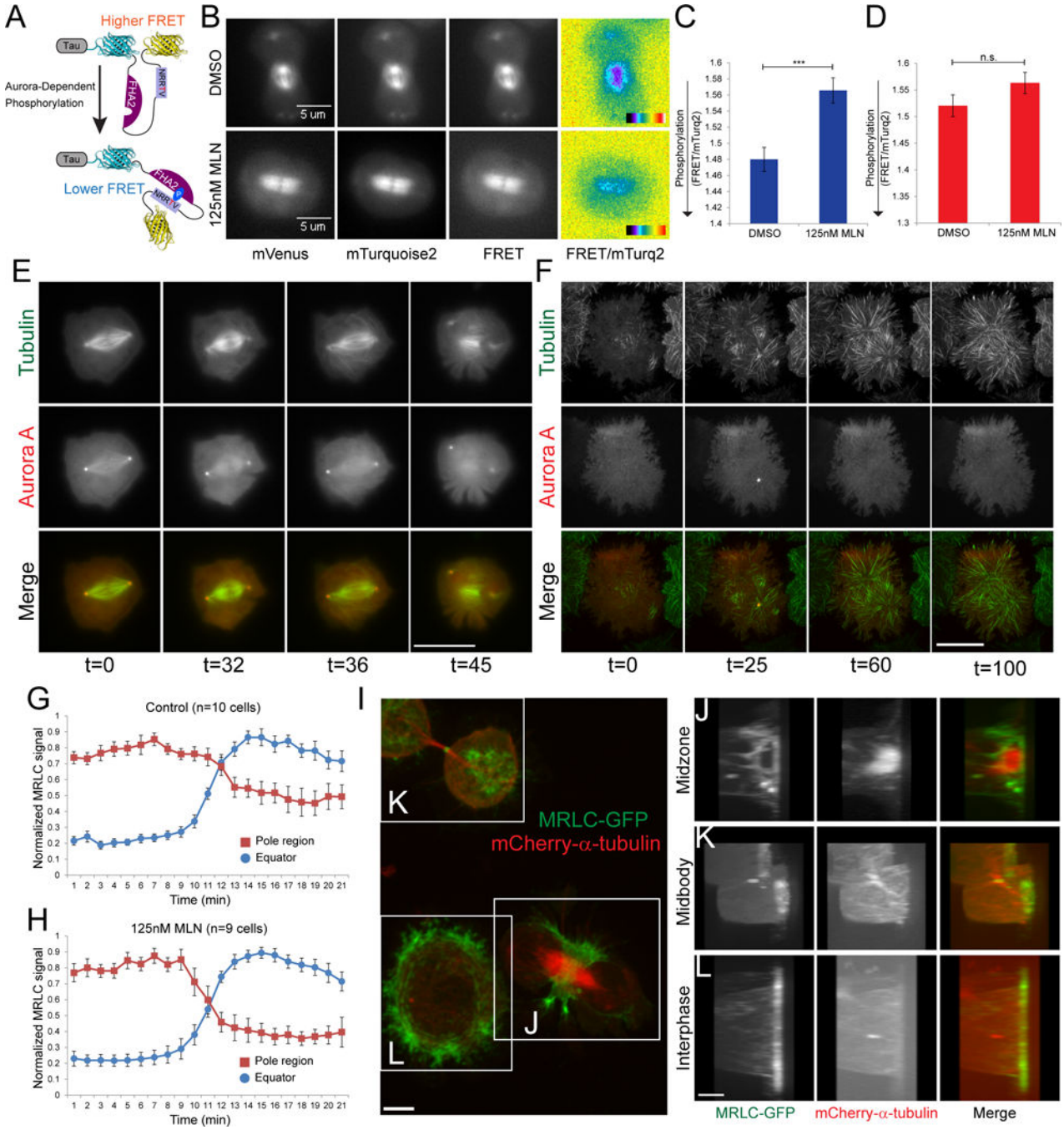

Figure 2. AAK contributes to the spindle midzone aurora kinase gradient but its inhibition does not significantly impact MRLC dynamics during cytokinesis

(A) A schematic of the MT-targeted FRET based phosphorylation sensor, highlighting the Threonine (T) residue that would be phosphorylated by aurora kinases. Phosphorylation causes a conformational change to this sensor that causes a decrease in FRET. **(B)** Representative images of the FRET reporter experiment quantified in (C). The FRET emission ratio images "FRET/mTurq2" are pseudo-colored with the color wedge spanning ratio values of 1.4 – 2.4. **(C)** Cells treated with 125nM MLN8237, which specifically

inhibits AAK activity, lowers the FRET emission ratio of the sensor at the spindle midzone, indicating it is less phosphorylated than in DMSO treatments. Quantifications are from 3 independent experiments. DMSO; n = 106 cells. 125nM MLN8237; n = 107 cells. **(D)** The FRET emission ratio of a non-phosphorylatable version of the sensor, in which the Threonine is mutated to Alanine, is not different between cells treated with DMSO and 125nM MLN8237. DMSO; n = 36 cells. 125nM MLN8237; n = 37 cells. **(E)** Still frames from wide-field time-lapse imaging of a high-expressing AAK-mCherry cell progressing from metaphase through cytokinesis onset. In the merged images tubulin is green and AAK is red. **(F)** Still frames from two-color TIRF imaging of an AAK-mCherry cell progressing from metaphase through cytokinesis onset. In the merged images tubulin is green and AAK is red. **(G)** MRLC is depleted from the pole region and accumulates at the cell equator during the metaphase to anaphase transition. The half change of myosin intensity at the equator happens, on average, 1 min before the loss of half of the myosin at the pole region. Quantifications are from 10 DMSO-treated cells. **(H)** Cells treated with 125nM MLN8237 do not exhibit significant changes in myosin dynamics during cell division relative to control cells, with the exception of one cell that failed cytokinesis. Quantifications are from 9 cells. **(I)** A maximum intensity projection of a spinning disk confocal image containing three cells at different stages of the cell cycle. MRLC is green, and tubulin is red. The z-stacks were used to reconstruct 3D images of the regions highlighted in the while boxes. **(J)** 3D reconstruction of a cell in late anaphase, after MRLC has already accumulated at the cleavage furrow. MLRC at the cell equator is forming a ring around the spindle. **(K)** 3D reconstruction of cells with a midbody between them. The MRLC has already constricted, but remains a ring around the midbody. **(L)** 3D reconstruction of an interphase cell. In the merged images (E-G) MLRC is green, and tubulin is red. Error bars are SEM. Scale bars are 5 μm (B, I-L) and 20 μm (E, F). Two-tailed Student's t-tests are reported: not significant (n.s.) = p-value > 0.05, *** = p-value < 0.0005.

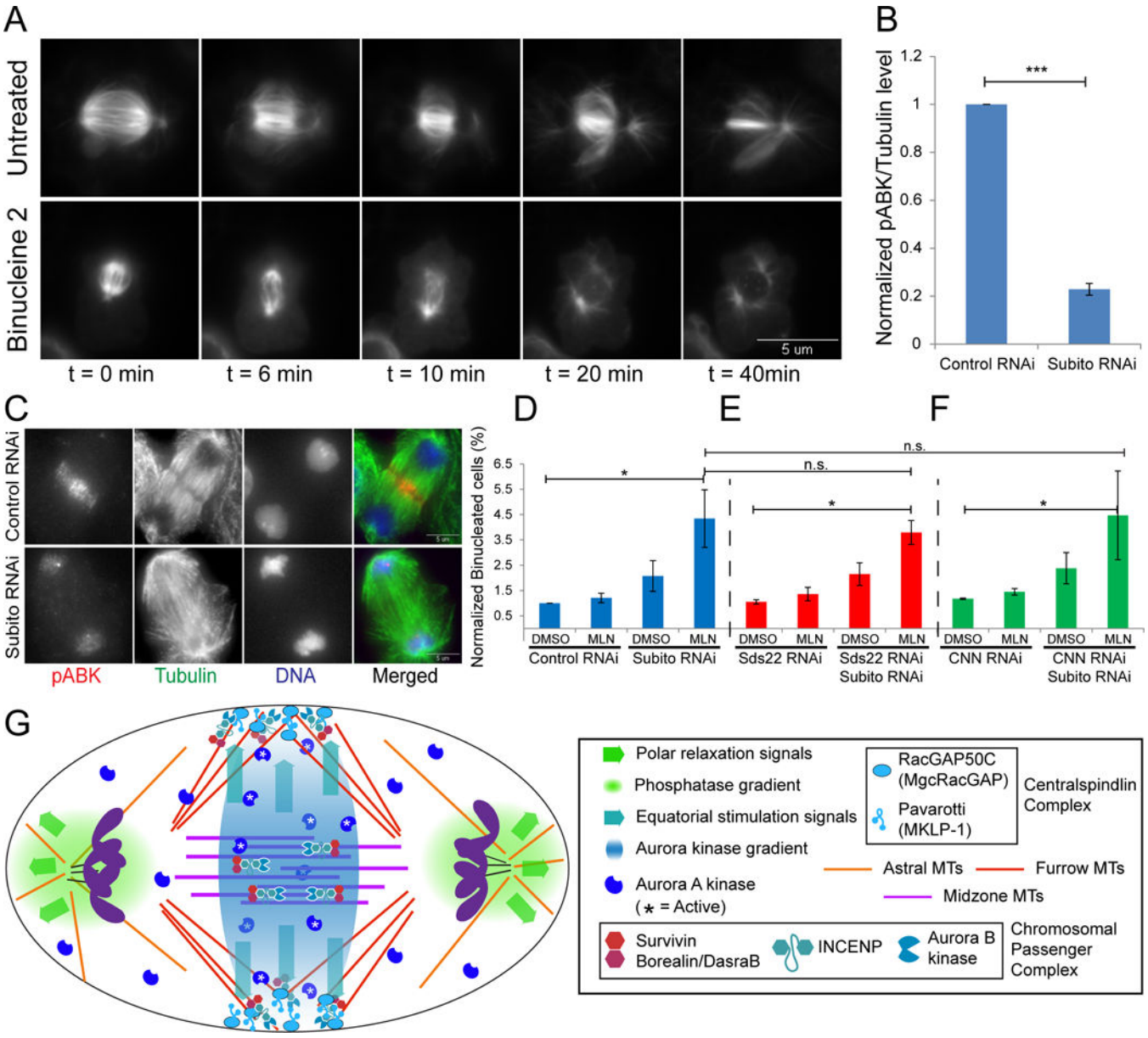

Figure 3. AAK and mABK together contribute to high fidelity cytokinesis and are not redundant with polar relaxation or centrosome-derived signals

(A) Still frames from wide-field time-lapse imaging of untreated (top) and 40μM binucleine-2 (bottom) treated S2 cells. **(B)** Subito depletion prevents the re-localization of pABK from the centromeres to the central spindle during the metaphase to anaphase transition. Quantifications are from 6 independent experiments. Control RNAi; n = 130 cells. Subito RNAi; n = 119 cells. **(C)** Representative images from experiments in (B). pABK staining remains at the centromeres in Subito depleted cells. In the merged images, pABK is red, tubulin is green, and DAPI is blue. **(D)** Quantification of binucleated cells (normalized to the baseline levels of control cells) in AAK inhibited, and Subito depleted plus and minus 125 nM MLN8237. AAK inhibition alone does lead to cytokinesis failure. Removal of mABK leads to a slight but not statistically significant increase in binucleated cells while

Subito RNAi in combination with 125nM MLN8237 treatment leads to a statistically significant increase in binucleated cells. Quantifications are from 5 independent experiments, Control RNAi + DMSO; n = 2134 cells, control RNAi + 125nM MLN8237; n = 2068 cells, subito RNAi + DMSO; n = 1500 cells, subito RNAi + 125nM MLN8237; n = 1837 cells. **(E)** Depletion of the Sds22-mediated phosphatase gradient that is required for polar relaxation does not lead to an increase in binucleated cells. Cells depleted of the midzone aurora gradient in addition to the phosphatase gradient exhibit the same phenotype as the Subito RNAi + MLN condition. Quantifications are from 3 independent experiments. Control+sds22 RNAi + DMSO; n = 1305 cells, control+sds22 RNAi + 125nM MLN8237; n = 1313 cells, subito+sds22 RNAi + DMSO; n = 1247 cells, subito+sds22 RNAi + 125nM MLN8237; n = 1305 cells. **(F)** Depletion of CNN does not increase the percentage of binucleated cells and exhibits the same phenotype as the Subito RNAi + MLN condition when combined with this treatment. Quantifications are from 2 independent experiments. Control+CNN RNAi + DMSO; n = 823 cells, control+CNN RNAi + 125nM MLN8237; n = 894 cells, subito+CNN RNAi + DMSO; n = 958 cells, subito+CNN RNAi + 125nM MLN8237; n = 931 cells. All data points were normalized to the control or single RNAi + DMSO condition. **(G)** A model highlighting three pathways that regulate positioning of the cleavage furrow. Error bars are SEM. Scale bars are 5μM. Two-tailed Student's t-tests are reported: not significant (n.s.) = p-value < 0.05, * p-value = < 0.05, *** = p-value <0.0005

Table 1

	Primer Sequence (5′→3′)
Aurora A RNAi F	TAATACGACTCACTATAGGGATGTCCCATCCGTCTGACCA
Aurora A RNAi R	TAATACGACTCACTATAGGGTTGCCAAACTTGCCCCGTCC
Subito RNAi F	TAATACGACTCACTATAGGGCTGAAGCTAATCAATGGCAGC
Subito RNAi R	TAATACGACTCACTATAGGGTTTTCTGAACTGTACTGGCCG
CNN RNAi F	TAATACGACTCACTATAGGGCTATGGGAGAAAAATCGTGAGG
CNN RNAi R	TAATACGACTCACTATAGGGTCTTTCCTCTGTCCTTCTGAGC
Sds22 RNAi F	TAATACGACTCACTATAGGGAGAACTTGTCCAGCCTGAAA
Sds22 RNAi R	TAATACGACTCACTATAGGGTTCTTGGCCAAGTCGAGGGT

Table 2

	No expression	FL Tau FRET-expressing
Growth Velocity (μm/min)	4.57	4.21
Shrink Velocity (μm/min)	5.56	5.34
Rescue Frequency (s^{-1})	0.014	0.014
Catastrophy Frequency (s^{-1})	0.057	0.06